Research Notes: Tabak-Rinzel, eupnea, sigh, and calcium dynamics

Greg Conradi Smith, Daniel Scott Borrus, Christopher Del Negro

January 4, 2021

An activity model of episodic bursting

We model the eupnea subsystem in a manner similar to Tabak and Rinzel (**?**). In the original Tabak-Rinzel model, the ODE representing network activity (firing rate) takes the form $\tau_a da/dt = a_\infty(w \cdot s \cdot d \cdot a) - a$ where s and d represent synaptic depression operating on a slow and fast time scales.

The steady state activity is the following sigmoidal function of synaptic input (x): $a_\infty(x) = [1 + e^{4(\theta_a - x)/k_a}]^{-1}$.

Fast synaptic depression leads to oscillatory dynamics during the active phase of each burst. These oscillations do not occur in our case, so the ODEs that are our starting point are $\tau_a da/dt = a_\infty(w \cdot s \cdot a) - a$ and $\tau_s ds/dt = s_\infty(a) - s$ where the steady state activity (firing rate) is the following sigmoidal function of synaptic input (x): $a_\infty(x) = [1 + e^{4(\theta_a - x)/k_a}]^{-1}$. Similarly, the steady state synaptic depression is a sigmoidal function of network activity: $s_\infty(a) = [1 + e^{4(\theta_s - a)/k_s}]^{-1}$. Thus, our two state variables can be written

$$\tau_a \frac{da}{dt} = a_\infty(w \cdot s \cdot a) - a \tag{1}$$

$$\tau_s \frac{ds}{dt} = s_\infty(a) - s \tag{2}$$

where a is the network activity and s accounts for the dynamics of synaptic depression. Note that when $s = 0$, the system is fully depressed. The steady state functions a_∞ and s_∞ are given by

$$a_\infty(x) = \frac{1}{1 + e^{4(\theta_a - x)/k_a}} \tag{3}$$

$$s_\infty(x) = \frac{1}{1 + e^{4(\theta_s - x)/k_s}} \tag{4}$$

Note: When k_a is positive (negative), a_∞ is a monotone decreasing (increasing) function of x, and similarly for k_s/s_∞. The 4 that appears in Eqs. 3 and 4 makes k_a and k_s the inverse of the slope of a_∞ and s_∞ at the half-max.

Fig. 1 shows that depending on the strength (gain) of recurrent excitation, denoted by w, the network activity can have 1–3 steady states. For intermediate values of w the excitatory network is bistable.

The a and s nullclines are given by $a = a_\infty(w \cdot s \cdot a)$ and $s = s_\infty(a)$. The first expression is implicit, but it can be written explicitly by viewing s as a function of a:

$$a \text{ nullcline:} \quad a = a_\infty(w \cdot s \cdot a) \Longrightarrow s = \frac{4\theta_a - k_a \ln\left[(1-a)/a\right]}{4wa} .$$

The system can be configured into two unique forms of excitability, depending on the parameters used. Fig. 2 shows nullclines with two parameter sets corresponding to type 2 (left) and type 1 (right) excitability.

As we adapt this model to represent a population of firing neurons, it will be helpful to assign realistic units to the firing rate, a. Rather than a representing the fraction of firing cells, we assign a units of spikes per neuron per second. When this is the case, a can be greater than 1, however the behavior of the a nullcline doesn't change that much. When $\lim_{x\to\infty} a_\infty(x) = a_{max} \neq 1$, the equation for the a nullcline is

$$a \text{ nullcline:} \quad a = a_\infty(w \cdot s \cdot a) \Longrightarrow s = \frac{4\theta_a - k_a \ln\left[(a_{max}-a)/a\right]}{4wa} .$$

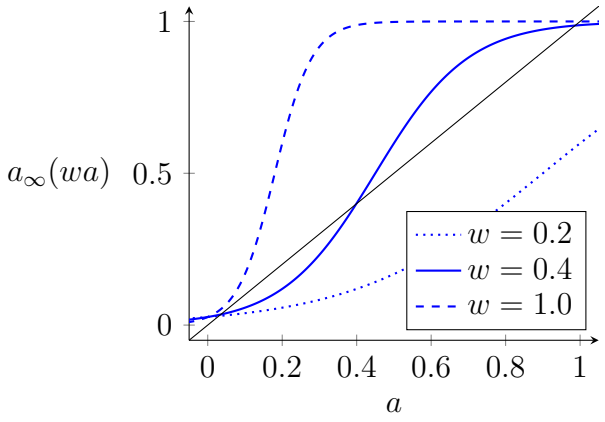

Figure 1: For intermediate values of w the excitatory network is bistable. Synaptic depression is off ($s = 1$). Parameters: $\theta_a = 0.18$, $k_a = 0.2$

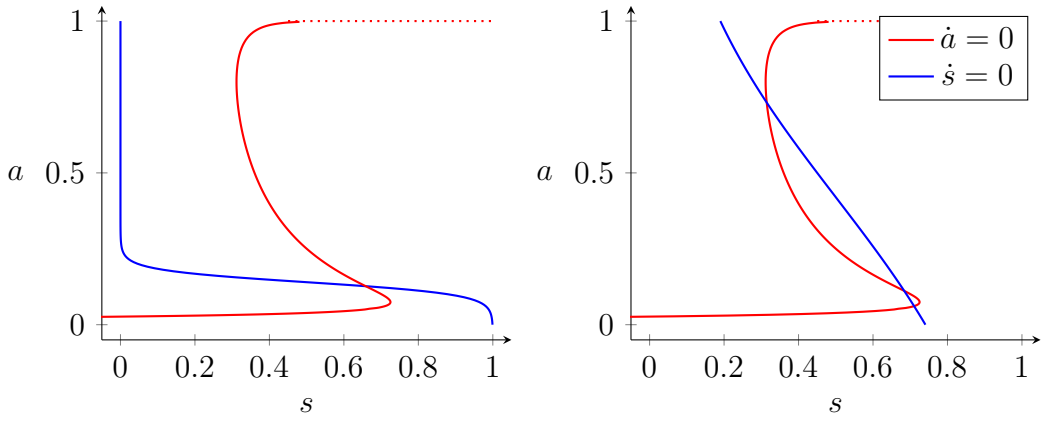

Figure 2: Nullcines for the modified Tabak-Rinzel model. Left: Type 2 oscillations; $\theta_s = 0.14$, $k_s = -0.08$. Right: Type 1 excitability; $\theta_s = 0.42$, $k_s = -1.6$. Other parameters: $w = 1$, $\tau_a = 10$, $\theta_a = 0.18$, $k_a = 0.2$.

Noise

So far we have assumed deterministic dynamics. Intrinsic stochastic dynamics of the excitatory network is modeled by additive Gaussian white noise with state-dependent variance to Eq. 1. The model is now written

$$\tau_a \frac{da}{dt} = a_\infty(w \cdot s \cdot a) - a + \hat{\xi}_a(a(t)) \tag{5}$$

$$\tau_s \frac{ds}{dt} = s_\infty(a) - s \tag{6}$$

The noise term has mean zero, i.e., $\langle \hat{\xi}_a \rangle = 0$. The variance of the Gaussian white noise is derived by considering the rates of the forward and reverse elementary processes implied by the deterministic ODE for the network activity. Consider the deterministic part of Eq. 1:

$$\frac{da}{dt} = \frac{a_\infty(wa) - a}{\tau_a}$$

where we note that $\lim_{x \to -\infty} a_\infty(x) = 0$ and write a_{max} for the limit of $a_\infty(x)$ as $x \to \infty$. Defining

$$\tau_a = \frac{1}{\alpha + \beta} \quad \text{and} \quad a_\infty = \frac{\alpha}{\alpha + \beta} a_{max}$$

we have

$$\alpha = \frac{a_\infty}{a_{max}\tau_a} \quad \text{and} \quad \beta = \frac{a_{max} - a_\infty}{a_{max}\tau_a}$$

Thus Eq. 1 can be written as

$$\frac{da}{dt} = \alpha(a_{max} - a) - \beta a$$

This is consistent with the elementary processes shown in this diagram:

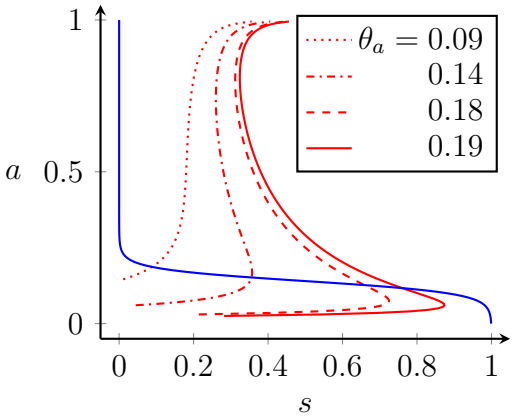

This leads to the following expression for the two-time covariance

$$\langle \hat{\xi}_a(t) \hat{\xi}_a(t') \rangle = \gamma_a(a, s)\delta(t - t')$$

where

$$\gamma_a(a, s) = \frac{1}{N}\left[\alpha \cdot (a_{max} - a) + \beta \cdot a\right] = \frac{1}{N a_{max}\tau_a}\left[a_\infty \cdot (a_{max} - a) + (a_{max} - a_\infty)a\right] \tag{7}$$

Figure 3 describes the size of the fluctuations as a function of the activity level.

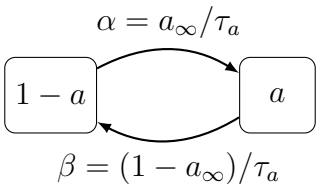

Figure 3: Size of fluctuations as given by Eq. 7. The size of the noise depends on the network firing rate a and synaptic depression s. Other parameters are the default values: $\theta_a = 0.18$, $k_a = 0.2$, $w = 1$.

System limitations arising from one slow variable

Our current system has one fast variable, a the network firing rate, and one slow variable, s the average synaptic depression in the network. With this fast-slow system we are able to generate network oscillations. Figure 4B depicts the trajectories of a and s when the system is configured for type 2 excitability. Here, the oscillations arise from a supercritical-hopf bifurcation (HB), and the appearance of a stable limit cycle. (should we include the bif. diagram?)

How well does this configuration of the model match with what we see in the preBötC experimentally?

The timing between each burst event is normally distributed, just like it is in the biology. The events are normal distributed because membrane noise either increases or decreases the total time synaptic depression can recover. However, this will lead to a problem with burst size.

We can see the noise manifest in the system at the bottom knee of the a nullcline. Now, each burst has a slight variation in the magnitude of its synaptic depression. This proves to be critical to the behavior of the system. If a burst is delayed, then the synaptic depression term recovers to a greater degree, and the ensuing burst will be larger. Ultimately, this leads to a phenomenon whereby bursts with longer preceding intervals have a larger burst area. There is a correlation between preceding interval and burst size. This has consequences for bursts that are initiated prematurely. Bursts that are "kicked" into the limit cycle early will ultimately terminate early, because synaptic depression hasn't fully recovered, and so ends the burst early. This is not observed experimentally.

First, there is no relationship between the preceding interval and the burst amplitude or area experimentally. (NEED FIGURE). Second, as was shown by CDN 2009 (FIX), there is a refractory period after a preBötC burst during which another network burst cannot be elicited. After that refractory period has expired, a burst can be evoked but the amplitude and area are not dependent on the time since the previous burst or the end of the refractory period. In the type-2 excitability configuration, burst events in the model will always depend on the magnitude of synaptic depression recovery. This problem can be resolved when we shift the model into type-1 excitability.

Figure 4B depicts the system in type-1 excitability. Here the system is subcritical to a saddle-node on an invariant circle (SNIC) bifurcation. Now the synaptic depression recovers to a maximum value before every burst. The burst size is no longer dependent on the duration of the preceding inter-event interval. Because the system is subcritical, it will not fire without some sort of noise. Membrane noise drives the system over the threshold, and triggers an event. Herein lies another problem.

The membrane noise is driven by a Wiener process, or brownian motion. As we wait for the noise to integrate above some threshold, we are waiting for a random event with some known probability to occur. This is Poisson process, and the timing between successive events will follow an exponential distribution. Indeed, in our model in a type-1 configuration, the timing between burst events appears to be exponentially distributed (after some minimal time). We know breaths are not exponentially distributed *in vivo*. That would be a terrifying

phenomenon. We can also show burst events are not exponentially distributed in the preBötC *in vitro*. (FIGURE)

Thus we are at an impasse with our two variable model. In the type-2 configuration, the timing between the events is normally distributed, but there is an undesirable relationship between the size of the burst events and the duration of the preceding interval. In the type-1 configuration, similar to the biology, there is no relationship between burst size and the preceding interval. However, here the timing between the events is exponentially distributed, which does not represent the biology. From here, in order to bring our model into agreement with what we observe physiologically, we reasoned we needed an additional slow variable.

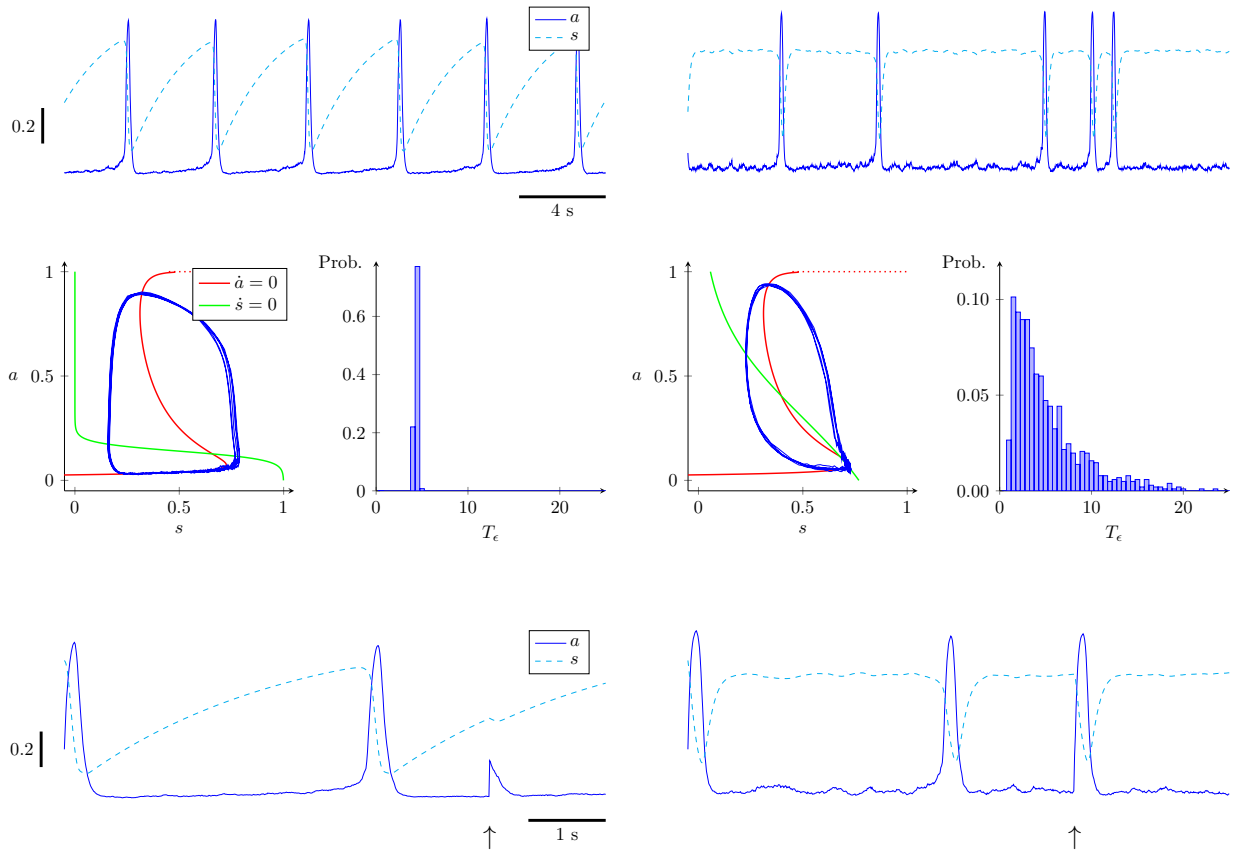

Figure 4: Draft figure for our argument that the eupnea model requires two slow variables.

The eupnea model

We model the eupnea subsystem using the following modifications of the Tabak-Rinzel-like model presented in the previous section. However, we include both synaptic depression (s) and cellular adaptation (θ). The ODEs for our modification of the Tabak-Rinzel model are

$$\tau_a \frac{da}{dt} = a_\infty(w \cdot s \cdot a - \theta) - a + \hat{\xi}_a(a(t)) \tag{8}$$

$$\tau_s \frac{ds}{dt} = s_\infty(a) - s \tag{9}$$

$$\tau_\theta(a) \frac{d\theta}{dt} = \theta_\infty(a) - \theta \tag{10}$$

where the variable θ is an adaptive threshold for the activity as a function of synaptic input. The steady state functions a_∞ and s_∞ are given by Eqs. 3 and 4. The steady-state function θ_∞ is analogous:

$$\theta_\infty(x) = \frac{1}{1 + e^{4(\theta_\theta - x)/k_\theta}} \,. \tag{11}$$

The logic behind including cellular adaptation is described in the section above. In brief, recovery of synaptic depression happens long before the end of the silent phase, therefore there must be a second low variable. The dependence of τ_θ on the activity level is chosen to be

$$\tau_\theta(x) = \frac{\tau_\theta^{max} - \tau_\theta^{min}}{1 + e^{4(\theta_{\tau_\theta} - x)/k_{\tau_\theta}}} + \tau_\theta^{min} \,. \tag{12}$$

This is important because the cellular adaptation needs to happen quickly in the active phase (when a is large), but recover slowly during the silent phase (when a is small). Figure 5 demonstrates the three state system undergoing oscillations. Synaptic depression terminates the bursts, and the recovery of the adaptation variable (θ) determines the timing of the subsequent burst.

The mathematical model for eupnea generation is inline with what we observe biologically. The timing between the events in normally distributed. And there is no relationship between the preceding interval and the size of the subsequent burst. (ADD TWO MORE FIGURES HERE DB).

Table 1 describes the default parameters used for the eupnea subsystem.

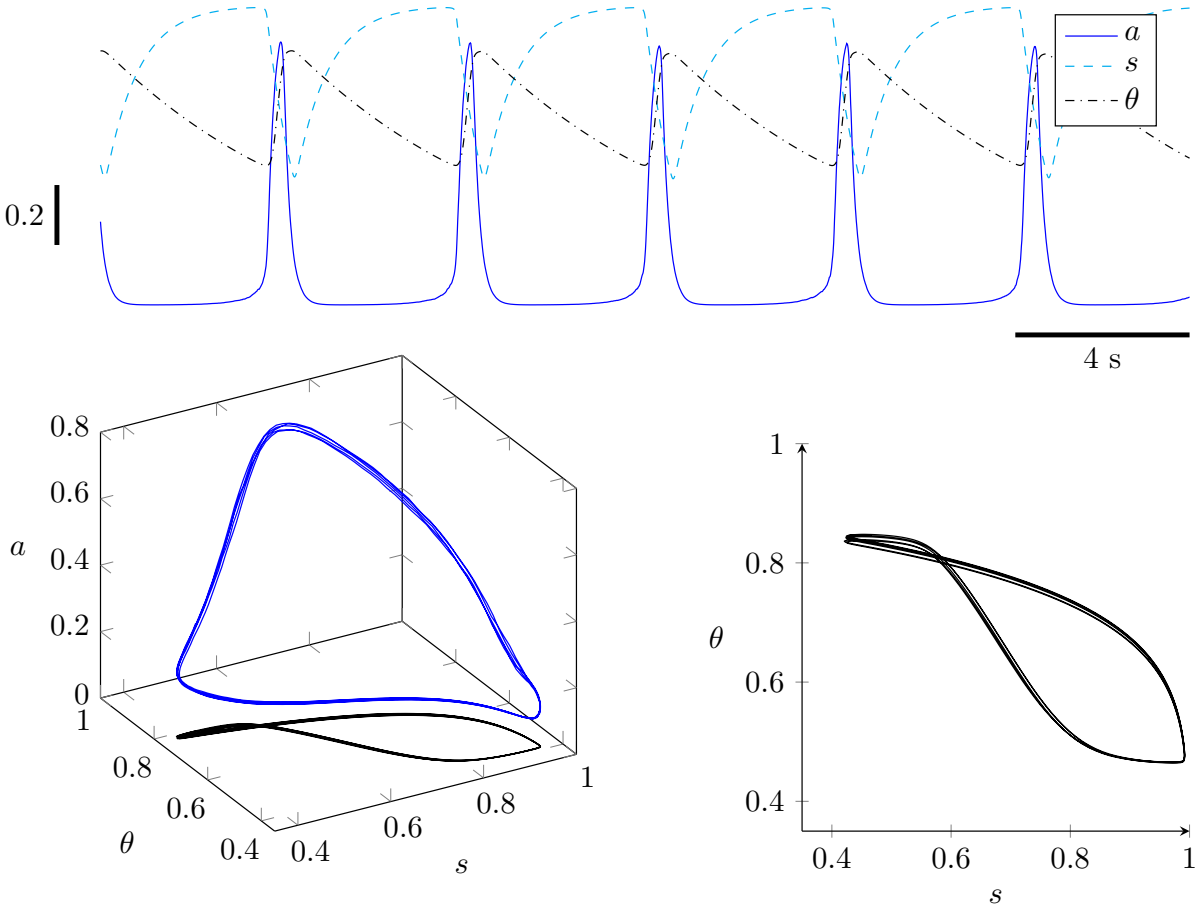

Figure 5: Draft figure showing Tabak-Rinzel like model with two slow variables (s and θ).

Symbol	Definition	Value	Units
w	network connectivity	1	-
θ_a	average firing threshold (half activation)	$[-0.3, 0.1]$	
k_a	reciprocal of slope of a_∞ at half activation	0.2	
τ_a	network recruitment time constant	0.15	
θ_s	half activation of s	0.14	
k_s	reciprocal of slope of s_∞ at half activation	-0.08	
τ_s	time constant of synaptic depression	0.75	
θ_θ	half activation of θ	0.15	
k_θ	reciprocal of slope of θ_∞ at half activation	0.2	
τ_θ^{max}	maximum of time constant of cellular adaptation	6	
τ_θ^{min}	minimum of time constant of cellular adaptation	0.15	
θ_{τ_θ}	half max of $\tau_\theta(a)$	0.3	
k_{τ_θ}	reciprocal of slope of $\tau_\theta(a)$ at half activation	-0.5	

Table 1: Description of parameters for eupnea model and standard values.

The sigh model: calcium handling

Closed cell Ca^{2+} model with bistability

We propose the sigh rhythm emerges from intracellular Ca^{2+} dynamics. We borrow the template for modeling Ca^{2+} handling from Keizer and Levine 1996. Our description of the equations begins with a closed system, where the total calcium in the cell is fixed and calcium moves between the cytosol and intracellular Ca^{2+} stores, such as the ER.

$$\frac{dc}{dt} = [v_1 r_\infty(c) + v_2]\,(c_{er} - c) - \frac{v_3 c^2}{k_3^2 + c^2} \tag{13}$$

$$c_{er} = (c_{tot} - c)/\lambda \tag{14}$$

$v_1 r_\infty(c)$ describes Ca^{2+} leaving the ER via Ca^{2+}-induced-Ca^{2+}-release. v_2 describes passive Ca^{2+} leak from the ER to the cytosol. v_3 controls the rate of Ca^{2+} in the cytosol being pumped into the ER via SERCA pumps on the walls of the ER. The phase diagram for Eq. **??** is shown in Figure 6. Depending on the total calcium in the cell, there are 1–3 steady states for the Ca^{2+} subsystem.

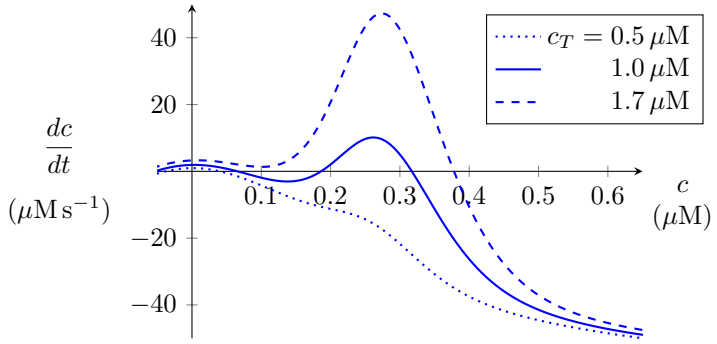

Figure 6: Closed cell model. Parameters: $\theta_m = 0.25$, $k_m = 0.04$, $\theta_h = 0.3$, $k_h = -0.06$, $\lambda = 0.15$, $v_1 = 40$, $v_2 = 0.5$, $v_3 = 120$, $k_3 = 0.3$.

Open cell Ca^{2+} model

Eqs. 13 and 14 can be modified to allow for Ca^{2+} fluxes across the plasma membrane. The Ca^{2+} concentration in the cell is no longer fixed. $\jmath_0$ controls the Ca^{2+} flux into the cytosol from outside the cell. v_4 regulates the rate Ca^{2+} is pumped out of the cell. The concentration of Ca^{2+} in the ER can be determined at any time by subtracting the total Ca^{2+} concentration by the Ca^{2+} concentration in the cytosol. λ accounts for the change in volume between the cytosol and ER.

$$\begin{aligned} \frac{dc}{dt} &= [v_1 f_\infty(c) + v_2]\,[c_{er} - c] - \frac{v_3 c^2}{\kappa_3^2 + c^2} + \jmath_0 - \frac{v_4 c^4}{\kappa_4^4 + c^4} \\ \frac{dc_{tot}}{dt} &= \jmath_0 - \frac{v_4 c^4}{\kappa_4^4 + c^4} \end{aligned}$$

where $c_{er} = (c_{tot} - c)/\lambda$ and

$$f_\infty(c) = \frac{1}{1 + e^{(\theta_m - c)/k_m}} \cdot \frac{1}{1 + e^{(\theta_h - c)/k_h}}$$

where $k_m > 0$ and $k_h < 0$. $f_(c)$ still describes the rate of Ca^{2+}-induced-Ca^{2+}-release and takes the form of a bell shaped curve. The dynamics of the open cell Ca^{2+} subsystem are described in Figure 7. Default parameters are written in Table 2.

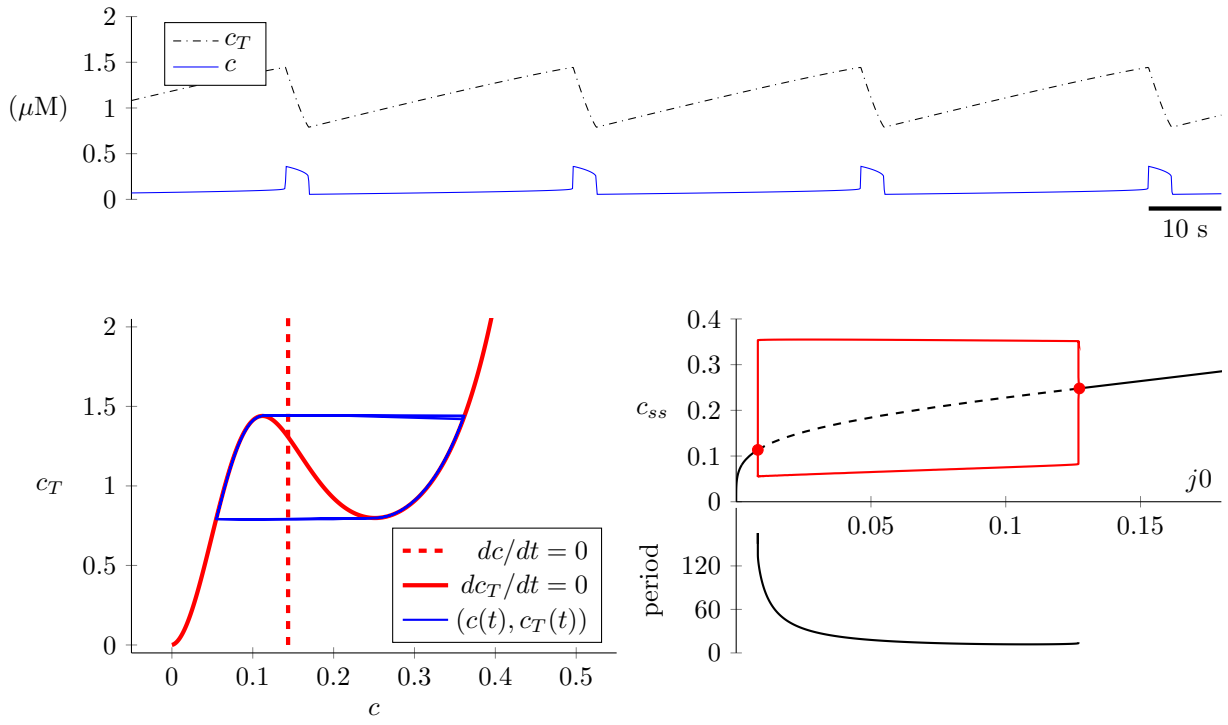

Figure 7: Open cell calcium dynamics. Calcium subsystem only.

Symbol	Definition	Value	Units
v_1	rate constant of calcium release	20	s^{-1}
v_2	rate constant of calcium leak	0.25	s^{-1}
v_3	maximum rate of SERCA pumps	60	$\mu\mathrm{M}\,\mathrm{s}^{-1}$
k_3	half maximum for SERCA pumps	0.3	$\mu\mathrm{M}$
n_3	Hill coefficient for SERCA pumps	2	-
λ	ER/cytosol effective volume ratio	0.15	-
θ_m	activation of intracellular calcium channels	0.25	$\mu\mathrm{M}$
k_m	reciprocal of slope of m_∞ at half maximum	0.04	-
θ_h	activation of intracellular calcium channels	0.3	$\mu\mathrm{M}$
k_h	reciprocal of slope of h_∞ at half maximum	-0.06	-
j_{in}^0	constant calcium influx rate	0.009	$\mu\mathrm{M}\,\mathrm{s}^{-1}$
j_{in}^1	calcium influx rate proportionality constant	0.02	$\mu\mathrm{M}\,\mathrm{s}^{-1}/activity$
v_4	maximum rate of PMCA pumps	0.4	$\mu\mathrm{M}\,\mathrm{s}^{-1}$
k_4	half maximum for PMCA pumps	0.3	$\mu\mathrm{M}$
n_4	Hill coefficient for PMCA pumps	4	-

Table 2: Description of parameters for calcium handling and standard values.

The Tabak-Rinzel-like activity model with calcium dynamics

We connected the eupnea and calcium subsystems to model the two simultaneous rhythms in preBötC, inspiratory and sigh breaths.

$$\begin{aligned}
\tau_a \frac{da}{dt} &= a_\infty(w \cdot s \cdot a - \theta, c) - a + \hat{\xi}(a) \\
\tau_s \frac{ds}{dt} &= s_\infty(a) - s \\
\tau_\theta(a) \frac{d\theta}{dt} &= \theta_\infty(a) - \theta \\
\frac{dc}{dt} &= [v_1 f_\infty(c) + v_2]\,[c_{er} - c] - \frac{v_3 c^2}{\kappa_3^2 + c^2} + \jmath_0 + \jmath_1 a - \frac{v_4 c^4}{\kappa_4^4 + c^4} \\
\frac{dc_{tot}}{dt} &= \jmath_0 + \jmath_1 a - \frac{v_4 c^4}{\kappa_4^4 + c^4}
\end{aligned}$$

where $c_{er} = (c_{tot} - c)/\lambda$ and

$$f_\infty(c) = \frac{1}{1 + e^{(\theta_m - c)/k_m}} \cdot \frac{1}{1 + e^{(\theta_h - c)/k_h}}$$

where $k_m > 0$ and $k_h < 0$. We assume that the steady state function a_∞ is 'boosted' by the intracellular calcium concentration, as follows:

$$a_\infty(x, c) = \frac{\lambda_a}{1 + e^{4(\theta_a - x)/k_a}} + \frac{\lambda_c}{1 + e^{4(\theta_c - c)/k_c}}$$

where λ_c is the contribution of intracellular Ca^{2+} to network activity. This is comparable to activation of a Ca^{2+}-activted Na^+ current (I_{CAN}). Activity is tied back into the Ca^{2+} subsystem via the $\jmath_1$ term. When activity is high, Ca^{2+} enters the cytosol at a rate proportional to $\jmath_1$. These terms are responsible for welding the two subsystems together.

The steady state cytosolic calcium concentration solves the implicit expression

$$0 = (v_1 + v_2 r_\infty(c)) \left(\frac{c_{tot} - c}{\lambda} - c \right) - \frac{v_3 c^2}{\kappa^2 + c^2} + \jmath_0 + \jmath_1 a - \frac{v_4 c^4}{\kappa_4^4 + c^4},$$

but this can be written as an explicit expression for c_{tot} as a function of c,

$$c_{tot} = (\lambda + 1)c - \frac{\lambda}{v_1 + v_2 r_\infty(c)} \left(-\frac{v_3 c^2}{\kappa^2 + c^2} + \jmath_0 + \jmath_1 a - \frac{v_4 c^4}{\kappa_4^4 + c^4} \right)$$

. The steady state total calcium concentration can also be calculated.

$$\begin{aligned}
0 &= \jmath_0 + \jmath_1 a - \frac{v_4 c^4}{\kappa_4^4 + c^4} \\
c &= \left(\frac{\kappa_4^4 (\jmath_0 + \jmath_1 a)}{v_4 - \jmath_0 + \jmath_1 a} \right)^{1/4}
\end{aligned}$$

Trajectories of the entire system are shown in Figure 8. The faster eupnea oscillation and the slower sigh oscillation run in parallel.

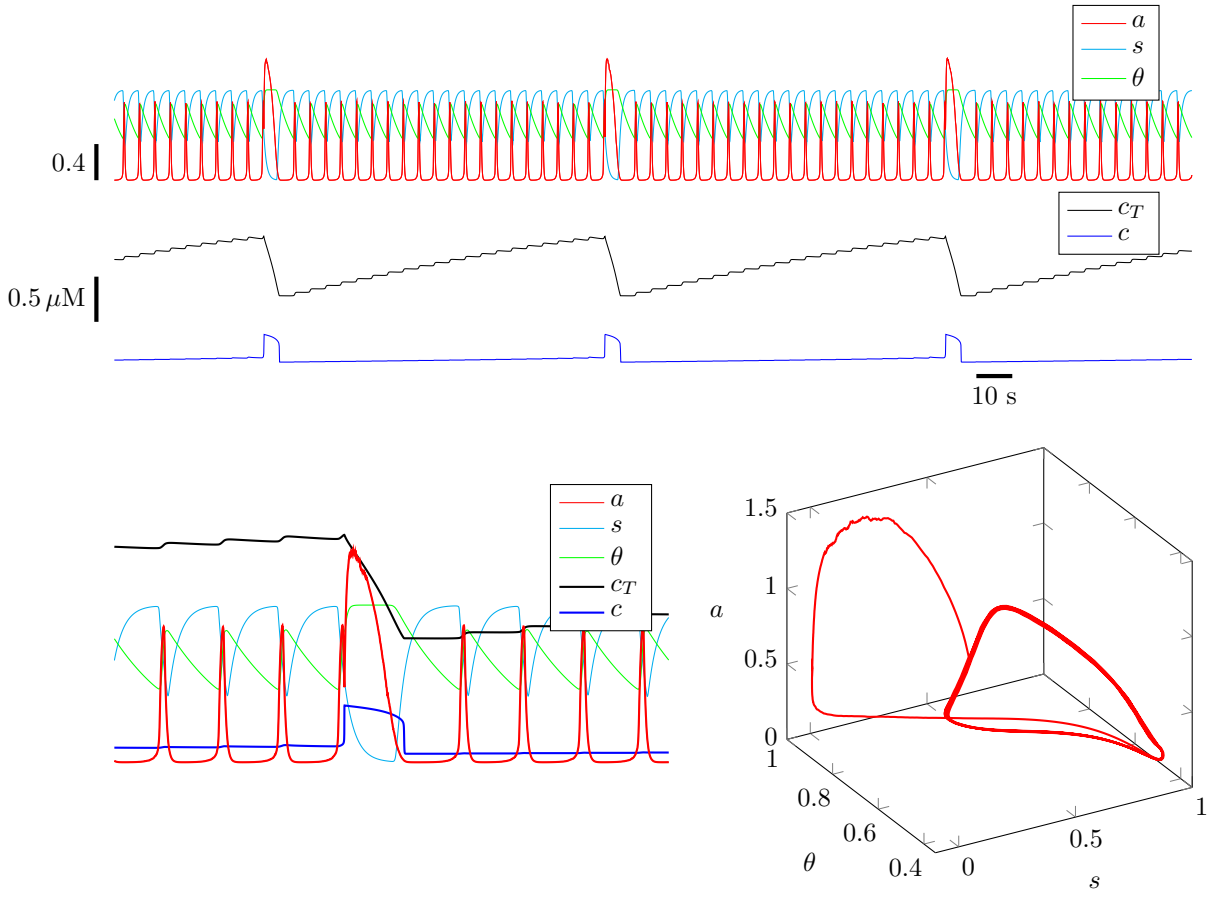

Figure 8: Draft figure of open cell model showing eupnea and sigh.

Eupnea and Sigh Voltage Dependence - Testable prediction #1

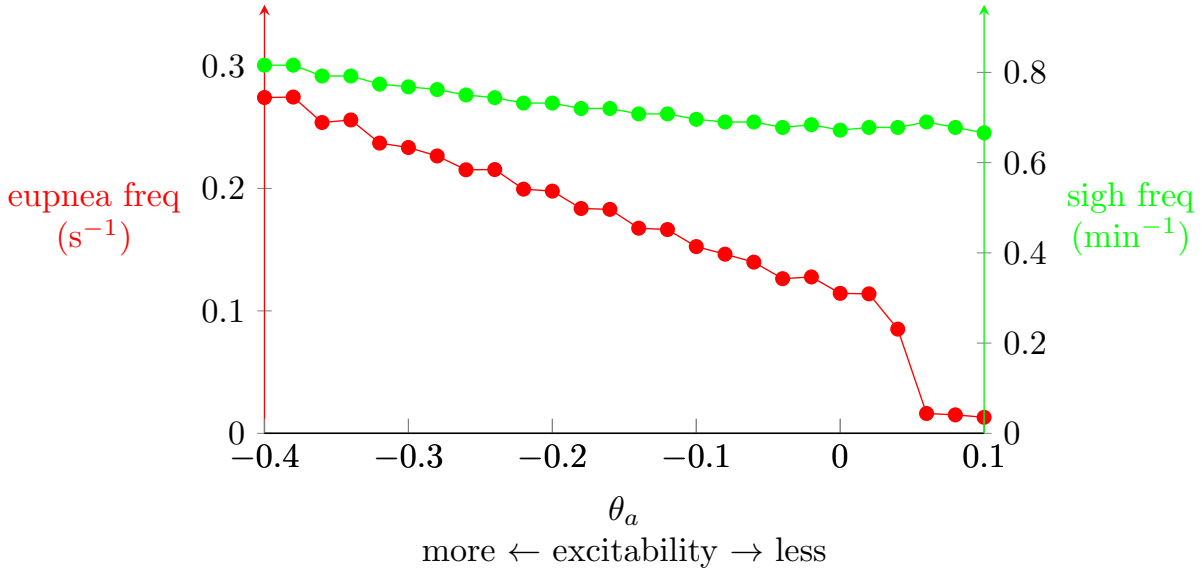

Figure 9: How excitability influences eupnea and sigh frequency.

Bombesin-like peptide modulating sigh frequency – Testable predicition #2

Calcium influx and coupling strength vs. eupnea/sigh timings – Testable prediction #3

High j0 should lead to faster Ca oscillations, and sighs – Testable prediction #4

Problem with this is, Δ Ca will influence eupnea frequency, which has a small, but non zero effect on sigh frequency.

Larger bursts will lead to high Ca influx during each eupniec burst, increasing sigh freq and increasing coupling– Testable prediction #5

block Glia (purinergic?) signaling

visualizing ER Ca fluxes with fluorescent indicators

SCRAPS

Jacobian of Tabak-Rinzel-like model

If τ_s is a constant, then the Jacobian of Eqs. 8 and 9 is

$$J(a,s) = \begin{pmatrix} \left[wsa'_\infty(wsa) - 1\right]/\tau_a & waa'_\infty(wsa)/\tau_a \\ s'_\infty(a)/\tau_s & -1/\tau_s \end{pmatrix}$$

where the steady state functions a_∞ and s_∞ are given by

$$\begin{aligned} a'_\infty(\theta) &= -4\frac{e^{4(\theta_a-\theta)/k_a}/k_a}{\left(1+e^{4(\theta_a-\theta)/k_a}\right)^2} \\ s'_\infty(\theta) &= -4\frac{e^{4(\theta_s-\theta)/k_s}/k_s}{\left(1+e^{4(\theta_s-\theta)/k_s}\right)^2} \end{aligned}$$

The condition for stability is $\operatorname{tr} J < 0$ and $\det J > 0$.

a_∞ with three inflection points

$N\tau_a(a_\infty - 2a_\infty a + a)$

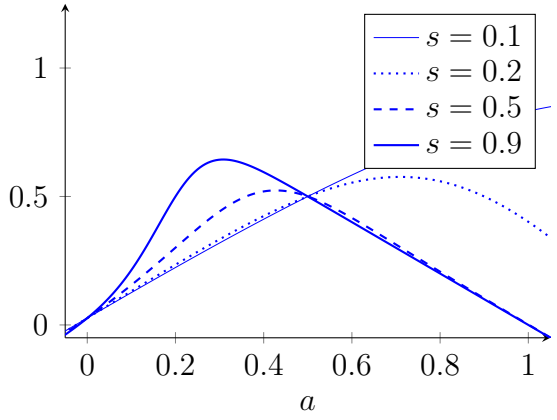

Figure 10: Parameters: $w = 0.4$, $\theta_a = 0.1$, $k_a = 0.1$, $\theta_b = 0.3$, $k_b = 0.1$, $\lambda = 0.5$.

$$a_\infty(x) = \frac{1-\lambda}{1+e^{4(\theta_a-x)/k_a}} + \frac{\lambda}{1+e^{4(\theta_b-x)/k_b}}$$

Constraining the new noise term - 4/23/20

What is the correct amount of noise for our model? Currently, the only noise in the model is network activity fluctuations driven by a stochastic process in the activity ODE a. The

equation for the a ODE is written (in the code):

$$\dot{a} = \frac{a_\infty - a}{\tau_a} + \texttt{randn} \cdot \texttt{dt}\sqrt{1/\texttt{dt}/N/\tau_a/a_{max} \cdot [a_\infty \cdot (a_{max} - a) + (a_{max} - a_\infty)a]}$$

As N is our dial for the amount of noise in the system, the question is, what is an appropriate N for our system? One idea to set this parameter is to compare the duration of inter-event-intervals we observe in the biology. Then to match increase noise in our simulation until we have a similar distribution of inter-event-durations.

I used 7 field recordings experiments and calculated the mean, sd, and coefficient of variation (cv) of the burst intervals. All intervals excluded sigh events.

Date	μ	σ	c.v.
180215	6.0 s	1.9 s	0.32
180309	7.0 s	1.3 s	0.19
080322	5.7 s	0.9 s	0.16
180420	7.6 s	1.4 s	0.18
180430	7.7 s	2.8 s	0.36
180515	5.6 s	0.8 s	0.14
180518	3.4 s	0.7 s	0.22
Average	6.1 s	1.1 s	0.23 s

Note, if we calculate cv on the averages, it's closer to cv = 0.19. Now that we have a desired distribution of inter-event-intervals, we can see how close we can get our simulation to the real data. Figure 11 shows what happens when we modulate noise in the model, and how close we can get to the actual recordings. Table 3 holds the key statistics of this test.

n	∞	1000	100	50	20	1	10*
σ	0	0	0.1	0.1	0.2	1.2	0.5
μ	4.3	4.3	4.3	4.3	4.3	3.8	4.3
c.v.	0	0.01	0.02	0.03	0.04	0.31	0.11

Table 3: For last column *: λ_a decreased from 20 to 7 spikes/neuron/second

We find that as N decreases, and the noise gets larger, our cv for event intervals doesn't get very large. Once we have 20 neurons in the simulation, the variability in event timing is still too small. We don't see large variability in eupnea timing in the model like we see in physiological data. Question for Greg & me to think about,

- is it cheating to move N extremely low? Like < 1? Probably.

- Maybe a better idea is to introduce a second type of noise to the model... I know we discussed Ca^{2+} $noise, but that won't help with this discrepancy between observed data and simulated results.$

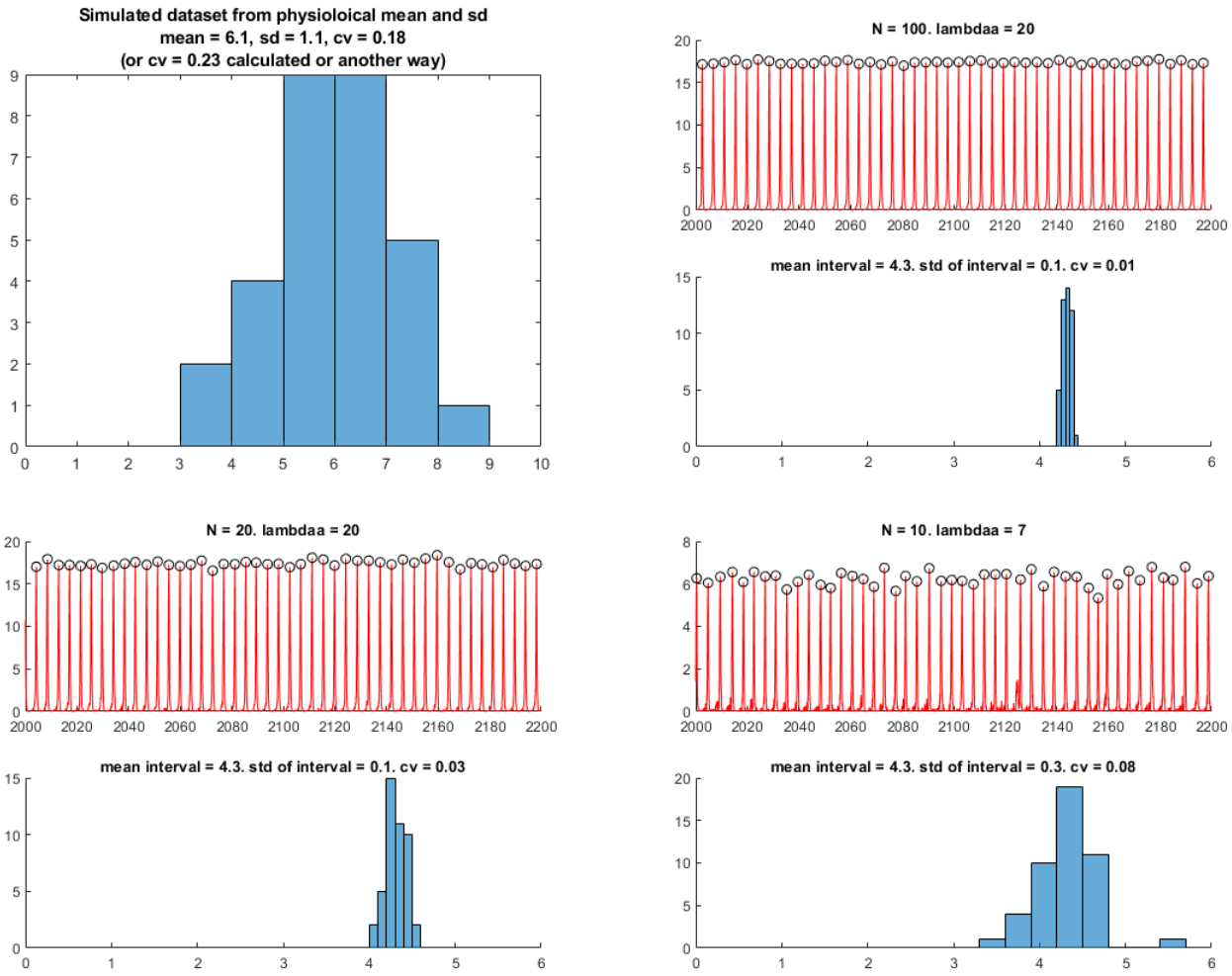

Figure 11: Top left: Simulated distribution from the physiological parameters. Notice the wide distribution in spike interval durations. Top right: In red, a trace of the simulated activity. Below in blue, the histogram showin interevent durations in seconds. Top right plot has the low noise, where $N = 100$. Bottom left has higher noise, but not high enough to have similar timing variability to physiological data. To get highest possible noise in physiological ranges, bottom right shows $N = 10$ and $\lambda_a = 7$. This gets a c.v. of only half the physiological norm.

s nulcline

$$\begin{aligned}
\tau_s \frac{ds}{dt} &= s_\infty(a) - s \\
0 &= \frac{1}{1 + e^{4(\theta_s - a)/k_s}} - s_{ss} \\
s_{ss} &= \frac{1}{1 + e^{4(\theta_s - a)/k_s}} \\
1 + e^{4(\theta_s - a)/k_s} &= \frac{1}{s_{ss}} \\
e^{4(\theta_s - a)/k_s} &= \frac{1}{s_{ss}} - 1 \\
4(\theta_s - a)/k_s &= \ln\left(\frac{1}{s_{ss}} - 1\right) \\
\theta &= \frac{k_s}{4} \ln\left(\frac{1}{s_{ss}} - 1\right)
\end{aligned}$$